Contrib Mineral Petrol (2007) 154:91–110
DOI 10.1007/s00410-007-0181-0

ORIGINAL PAPER

Archaean TTGs as sources of younger granitic magmas: melting of sodic metatonalites at 0.6–1.2 GPa

J. M. Watkins · J. D. Clemens · P. J. Treloar

Received: 4 November 2005 / Accepted: 8 January 2007 / Published online: 6 March 2007

Abstract Two natural, low K_2O/Na_2O, TTG tonalitic gneisses (one hornblende-bearing and the other biotite-bearing) were partially melted at 0.8–1.2 GPa (fluid-absent). The chief melting reactions involve the breakdown of the biotite and hornblende. The hornblende tonalite is slightly less fertile than the biotite tonalite, but melt volumes reach around 30% at 1,000°C. This contrasts with results of most previous work on more potassic TTGs, which generally showed much lower fertility, though commonly producing more potassic melts. Garnet is formed in biotite-bearing tonalitic protoliths at $P > 0.8$ GPa and at > 1.0 GPa in hornblende-bearing tonalitic protoliths. All fluid-absent experiments produced peraluminous granitic to granodioritic melts, typically with $SiO_2 > 70$ wt.%. For the biotite tonalite, increasing T formed progressively more melt with progressively lower K_2O/Na_2O. However, the compositions of melts from the hornblende tonalite do not vary significantly with T. With increasing P, melts from the biotite tonalite become less potassic, due to the increasing thermal stability of biotite. For the hornblende tonalite, again there is no consistent trend. Fluid-absent melting of sodic TTGs produces melts with insufficient K_2O to model the magmas that formed the voluminous, late, potassic granites that are common in Archaean terranes. Reconnaissance fluid-present experiments at 0.6 GPa imply that H_2O-saturated partial melting of TTGs is also not a viable process for producing magmas that formed these granites. The protoliths for these must have been more potassic and less silicic. Nevertheless, at granulite-facies conditions, sodic TTGs will produce significant quantities of broadly leucogranodioritic melt that will be more potassic than the protoliths. Upward abstraction of this melt would result in some LILE depletion of the terrane. Younger K-rich magmatism is unlikely to represent recycling of TTG crust on its own, and it seems most likely that evolved crustal rocks and/or highly enriched mantle must be involved.

Communicated by I. Parsons.

Electronic supplementary material The online version of this article (doi:10.1007/s00410-007-0181-0) contains supplementary material, which is available to authorized users.

J. M. Watkins · J. D. Clemens (✉) ·
P. J. Treloar
School of Earth Sciences and Geography, CEESR,
Kingston University, Penrhyn Rd, Kingston-upon-Thames,
Surrey KT1 2EE, UK
e-mail: j.clemens@kingston.ac.uk

Introduction–crustal melting and Archaean granites

Petrological, geochemical and isotopic studies have shown that most granitoid magmas contain major contributions from melts formed by anatexis of crustal materials during high-grade metamorphism. Other (more minor) components are mantle-derived, though their exact character and proportions are highly variable (see e.g. Patiño Douce 1999). Granitoid magmas emplaced at high crustal levels are initially H_2O-undersaturated (Clemens 1984). Clemens and Watkins (2001) demonstrated that the sort of granulite-facies metamorphism that produces granitic magmas takes place in the effective absence of a fluid phase. The high temperatures (>800°C) needed to partially melt the

crust can only be achieved in the upper amphibolite and granulite facies. Thus there is a strong inferred genetic link between granulite-facies metamorphism and granitic magma generation (e.g. Brown and Fyfe 1970; Fyfe 1973; White and Chappell 1977; Clemens 1990).

Granulite-facies partial melting, with melt removal, has been postulated as a major mechanism for internal differentiation of the continental crust (Wells 1981; Clemens 1990). Indeed, the restitic (melt-depleted) character of some granulite terranes is beyond dispute, and melt extraction has commonly been highly efficient (e.g. Guernina and Sawyer 2003; Barboza and Bergantz 2000). In theory, the LILE depletion commonly observed in granulites results from such melt removal. For post-Archaean rocks, this would require the granulite-facies lower crust to have a positive Eu anomaly, to balance the negative anomaly in the upper crust (Taylor and McLennan 1985). Since Archaean upper crustal rocks typically have no Eu anomalies, either partial melting of the lower crust was not a major mechanism for crustal differentiation in the Archaean (Taylor and McLennan 1985) or melting occurred outside the plagioclase stability field.

The first aim of the present work is to experimentally investigate processes of partial melting in ancient TTG (tonalite, trondhjemite and granodiorite) terranes, using rocks of the Lewisian Gneiss Complex of NW Scotland as a model for the more sodic protoliths. There is debate over the tectonic settings in which Archaean felsic magmatism and regional metamorphism occurred (e.g. Dziggel et al. 2002, and references therein). We assume that the pressures involved will not exceed those found in ordinary thickened continental crust (i.e. ≤1.2 GPa). The second aim is to investigate potential links between magma extraction, emplacement of late potassic granites and LILE depletion in deep crustal high-grade terranes.

Melting reactions investigated

Two sets of experiments were carried out. One set involved the relatively high-temperature, fluid-absent partial melting of TTG-series rocks in which the main melting reactions involve breakdown of biotite and hornblende. The other set involved lower-temperature, fluid-present (H_2O-saturated) partial melting of the same rocks. For a summary of these types of reactions, the reader should consult earlier works (e.g. Clemens 1990).

H_2O-dominated fluids can flux partial melting of quartzofeldspathic crustal rocks at relatively low temperatures, essentially at the wet haplogranite solidus. However, if fluid supply is limited, all the available H_2O would dissolve into the first melt fraction and the system would become fluid-absent. At near-solidus conditions, larger volumes of H_2O would allow larger melt volumes to be formed, while biotite and amphibole would remain stable, due to the small quantities of these phases involved in congruent wet solidus reactions such as:

$$\mathrm{Hbl/Bt} + \mathrm{Qtz} + \mathrm{Kfs/Pl} + \mathrm{H_2O} = \mathrm{melt}. \quad (1)$$

If metamorphic temperatures reached those of the incongruent fluid-present melting reactions, biotite and hornblende would decompose or be entirely consumed in reactions are similar to:

$$\mathrm{Hbl} + \mathrm{Qtz} + \mathrm{H_2O} = \mathrm{Cpx} + \mathrm{Opx} \pm \mathrm{Grt} + \mathrm{melt} \quad (2)$$

and

$$\mathrm{Bt} + \mathrm{Qtz} + \mathrm{Pl} + \mathrm{H_2O} = \mathrm{Opx} \pm \mathrm{Cpx} \pm \mathrm{Grt} + \mathrm{melt}. \quad (3)$$

Fluid-absent partial melting is the most likely process by which granulite-facies 'dehydration' occurs (e.g. Clemens and Watkins 2001). Such reactions involve incongruent breakdown of hydrous minerals (usually micas and amphiboles) to produce anhydrous restitic mineral assemblages and complementary H_2O-undersaturated melts. The most likely restite-producing reactions for partial melting of TTG-type source rocks are of the type:

$$\mathrm{Hbl} + \mathrm{Qtz} = \mathrm{Cpx} + \mathrm{Opx} \pm \mathrm{Grt} + \mathrm{Pl} + \mathrm{melt} \quad (4)$$

or, for the less abundant rocks in which biotite dominates:

$$\mathrm{Bt} + \mathrm{Qtz} + \mathrm{Pl} = \mathrm{Opx} \pm \mathrm{Grt} \pm \mathrm{Kfs} + \mathrm{melt}. \quad (5)$$

Previous work on fluid-absent melting of tonalites

Rutter and Wyllie (1988), Skjerlie and Johnston (1992), Singh and Johannes (1996a, b), Gardien et al. (1995, 2000), Castro (2004) and Patiño Douce (2005) all studied the fluid-absent partial melting of natural, broadly metatonalitic compositions. Figure 1 shows a plot of the normative compositions of the tonalitic starting materials used in previous studies (Table 1), as well as the rocks used in the present work (see below). The Rutter

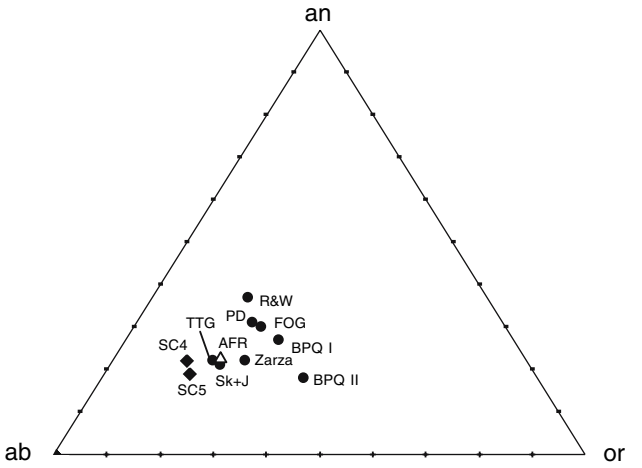

Fig. 1 Normative an-ab-or diagram showing the compositions of the starting materials used in previous tonalite partial melting experiments (Table 1), as well as the points representing the average Archaean felsic rock (*AFR*, Taylor and McLennan 1985) and the two starting materials used in the present study (SC4 and SC5). TTG = average TTG (Castro 1997, 2004), SK + J = F-rich metatonalite (Skjerlie and Johnston 1992), Zarza and FOG = biotite metatonalites (Castro 2004), PD = hornblende biotite tonalite (Patiño Douce 2005), R&W = tonalite (Rutter and Wyllie 1988), BPQ I and BPQ II = biotite-plagioclase-quartz metatonalites (Gardien et al. 2000)

and Wyllie starting material was intermediate, rather than silicic, and rather calcic, quite dissimilar to the average TTG (Table 1, Fig. 1). The unusual experimental design of Singh and Johannes (a large plagioclase crystal surrounded by a quartz–biotite mixture) does not permit calculation of the effective starting composition, though it must have been broadly tonalitic. Gardien et al. (1995) studied biotite–plagioclase–quartz gneisses (BPQI and BPQII) that are evidently meta-igneous (granodiorite and tonalite). However, these are rather too potassic to be models for TTG melting. The rock studied by Skjerlie and Johnston (1992, 1993) is a tonalite containing 20% fluorine-rich biotite and 2% hornblende. Its normalised composition (fluorine-free) is relatively similar to the average TTG but its melting behaviour is strongly influenced by the high fluorine content and the results are not directly applicable to Archaean TTG melting.

Castro (2004) performed fluid-absent melting experiments on two biotite metatonalite gneisses. His starting material FOG is less silicic and more mafic, and much more magnesian and potassic than the average Archaean felsic rock (Table 1, Fig. 1). The other rock (Zarza, Table 1) is, in many respects, a good model for the average Archaean felsic rock, though somewhat more potassic (Fig. 1). Castro also carried out a single experiment on a synthetic starting material with the composition of Condie's (1997) average

Table 1 Compositions (normalised 100% anhydrous) of experimental starting materials and average Archaean felsic rock (Taylor and McLennan 1985)

	Average Archaean felsic rock	Hbl metatonalite (SC4)	Bt metatonalite (SC5)	F-rich metatonalite (Skjerlie and Johnston 1992)	Metatonalite (Gardien et al. 2000)		Mafic tonalite (Rutter and Wyllie 1988)	Bt metatonalite (Castro 2004)			Mafic Hbl–Bt tonalite (Patiño Douce 2005)
					BPQ I	BPQ II		FOG	Zarza	Ave. TTG[b]	
SiO_2	69.7	69.28	70.64	68.55	65.42	69.70	60.10	65.00	68.65	70.03	61.55
TiO_2	0.5	0.35	0.29	0.52	0.68	0.83	0.80	0.78	0.52	0.34	0.90
Al_2O_3	15.8	16.14	16.30	14.95	16.61	12.68	18.53	17.16	16.30	15.22	17.09
FeO^a	3.1	2.56	2.09	4.69	4.65	6.48	5.80	3.43	3.75	3.53	5.93
MnO	0.15	0.03	0.02	0.06	0.05	0.12	0.11	0.10	0.03	0.00	n.d.
MgO	1.4	1.00	0.78	1.74	1.39	2.59	2.54	3.13	1.52	1.11	2.68
CaO	2.9	3.79	2.71	2.94	3.90	1.80	6.02	4.11	2.79	2.82	5.40
Na_2O	4.3	5.31	5.35	4.49	3.63	2.57	3.87	3.60	3.84	4.53	3.88
K_2O	2.2	1.54	1.82	2.06	3.45	3.24	2.23	2.68	2.60	2.42	2.57
K_2O/Na_2O	0.51	0.29	0.34	0.46	0.95	1.26	0.58	0.74	0.68	0.53	0.66
Mg#	45	41	40	40	35	42	44	62	42	36	51

Mg# = 100Mg/(Mg + Fe), *n.d.* not determined

[a] Total Fe as FeO

[b] Average Archaean TTG of Condie (1997)

Archaean TTG, very similar in composition to the average Archaean felsic rock given by Taylor and McLennan (1985), though a little less magnesian (Table 1). The melts derived from all these starting materials were granitic (s.s.). Very small melt proportions were produced (<10%), and only at $T > 900°C$. Castro concluded that fluid-absent partial melting of Archaean metatonalites is not a viable mechanism for the production of voluminous high-K granitic magmas.

Patiño Douce (2005) investigated the fluid-absent partial melting of a natural, relatively potassic, mafic, magnesian tonalite (Table 1, Fig. 1). Designed to model UHP partial melting of subducted continental crust, the experiments were carried out at pressures of 1.5–3.2 GPa and temperatures >900°C. Melt-producing reactions occurred by breakdown of phengitic mica and zoisite; the melts were leucogranitic and strongly peraluminous.

Based on these previous studies, it appears that metatonalites can yield a few tens of percent of melt at temperatures attainable in the crust (up to 1,000°C, Petford and Gallagher 2001). Many of the differences in melt production, between the different experiments, can be explained by variations in modal biotite and/or hornblende contents in the starting materials. However, the partial melting behaviour of the more common sodic TTG compositions has not been adequately investigated.

The present experiments

The partial melting behaviour of sodic metatonalites is important because, although much of Earth's early continental crust is inferred to have been composed of such rocks (Barker 1979; McGregor 1979), there have been essentially no previous experiments on appropriate compositions (see above and Fig. 1). We carried out experiments on two natural low-K_2O/Na_2O starting materials (SC4 and SC5, Table 2, Fig. 1). The chosen compositions are a little more sodic than the average Archaean TTG, and the results should be viewed as typical of this end of the compositional spectrum—a balance to the previous studies on more potassic rocks. Our results have implications for the origins of granites and LILE depletion in Archaean terranes and the fertility of sodic TTGs as magma sources.

Starting materials

SC4 is a hornblende tonalite with subsidiary biotite, and comes from the Rhiconich area in NW Scotland (British National Grid reference NC 255526). SC5 is a biotite tonalite from the area north of Laxford Bridge, also in NW Scotland (grid reference NC 2354900). SC4 and SC5 have similar bulk compositions (Table 2, Fig. 1), so the specific influence of mineralogy on partial melting behaviour could be examined. Specifically, since hornblende has a lower H_2O content than biotite, this should affect the relative fertilities of the two rocks under fluid-absent melting conditions. Whole-rock analyses were carried out by ICP-AES and ICP-MS, and mineral compositions were determined by EMPA. Table 2 shows the modal mineralogy, bulk-rock chemistry and CIPW norms of the two rocks, and Table 3 shows representative analyses of minerals. Biotites have Mg# = 55 in SC4 and 41 in SC5. The amphibole in SC4 is a hastingsitic hornblende with Mg# = 42. The F contents of the hornblendes and biotites in SC4 and SC5 are below the detection limits (~0.25 wt.%) of the electron probe (EDS) at Kingston. Plagioclase is An_{23} in both rocks. SC4 and SC5 both plot on the boundary between the tonalite and trondhjemite fields of Barker (1979) on a normative an-ab-or plot (see later, Fig. 7).

Run conditions

Fluid-absent experiments were carried out to model granulite- and upper amphibolite-facies metamorphism

Table 2 Major element analyses, CIPW norms and modal mineralogy of starting materials

wt. % Oxide	SC4	SC5	CIPW norm	SC4	SC5	Mode (wt.%)	SC4	SC5
SiO_2	68.98	70.12	q	21.68	24.04	Pl	57	58
TiO_2	0.35	0.29	c		0.60	Qtz	24	27
Al_2O_3	16.07	16.18	or	9.10	10.76	Kfs	7	6
FeO[a]	2.54	2.07	ab	44.93	45.27	Bt	3	9
MnO	0.03	0.02	an	15.66	13.44	Hbl	9	
MgO	1.00	0.77	di	2.65				
CaO	3.77	2.69	hy	5.32	5.34			
Na_2O	5.29	5.31	il	0.66	0.55			
K_2O	1.53	1.81						
H_2O	0.45	0.74	Mg#	41	40			
Total	100.00	100.00	K_2O/Na_2O	0.29	0.34			

Mg# = 100Mg/(Mg + Fe)

[a] Total Fe as FeO

Table 3 Representative mineral analyses for starting materials

	SC4					SC5			
	Pl	Hbl	Bt	Kfs	Ep	Pl	Bt	Kfs	Ep
SiO_2	63.90	42.00	37.33	65.68	37.49	62.83	36.84	63.96	36.53
TiO_2	0.00	0.88	1.57	0	0.11	0.00	3.64	0.00	1.49
Al_2O_3	23.95	11.15	15.64	18.18	23.73	23.77	15.97	18.83	20.15
Fe_2O_3					13.63				15.63
FeO[a]	0.00	20.47	18.62	0.22		0.00	22.33	0.00	
MnO	0.00	0.38	0.00	0.00	0.00	0.00	0.18	0.00	0.20
MgO	0.00	8.30	12.78	0.00	0.00	0.00	8.83	0.00	0.05
CaO	4.93	11.50	0.38	0.15	23.36	4.92	0.00	0.12	21.69
Na_2O	9.18	1.76	0.00	0.04	0.18	8.95	0.43	1.02	0.22
K_2O	0.11	1.47	9.90	16.38	0.00	0.14	9.76	14.77	0.02
Total	102.07	97.91	96.22	100.65	98.50	100.61	97.98	99.85	95.98
Si	2.78	6.43	5.62	2.98	2.95	2.77	5.52	2.97	3.01
Ti		0.10	0.18		0.01		0.41		0.09
Al	1.23	2.01	2.78	1.01	2.20	1.23	2.81	1.03	1.95
Fe^{3+}					0.90				1.08
Fe^{2+}		2.62	2.34	0.01			2.80		
Mn		0.05					0.02		0.02
Mg		1.89	2.87				1.97		0.01
Ca	0.23	1.89		0.01	1.97	0.23		0.01	1.91
Na	0.77	0.52	0.11	0.04	0.03	0.76	0.13	0.09	0.04
K	0.01	0.29	1.90	0.95		0.01	1.87	0.88	0.00
O	8.00	22.93	22.00	8.00	12	8.00	22.00	8.00	12.00
Cation sum	5.02	15.80	15.80	5.00	8.06	5.01	15.53	4.98	8.09
	An_{23} Ab_{76}	Mg# = 42	Mg# = 55	Or_{95}		An_{23} Ab_{76}	Mg# = 41	Or_{90}	

[a] Total Fe as FeO except for epidote which is calculated with total Fe as Fe_2O_3

of TTGs. H_2O-saturated experiments were designed to model conditions that might occur in fluid-present, high-grade metamorphism. Fluid-absent experiments were carried out mainly at 0.8 GPa, with reconnaissance experiments at 1.0 and 1.2 GPa, and some intermediate pressures, corresponding to the range of pressures common in granulite-facies metamorphism of Archaean terranes. H_2O-saturated experiments were carried out at 0.6 GPa.

The fluid-absent experiments (800–1,000°C) constrain the position of the solidus, the temperature of biotite breakdown in SC5, hornblende breakdown in SC4, and the effects of T on garnet stability. For the H_2O-saturated experiments, temperatures were 680–730°C, slightly above the haplogranite solidus. This enabled us to locate the 'wet' solidus and collect data on the compositions of H_2O-saturated melts of sodic metatonalites.

Experimental methods

Starting rocks were ground, in agate mills, to ~5 μm, dried at 110°C and stored in a vacuum desiccator over silica gel. For each experiment, one end of an annealed Au capsule (3 mm OD by 0.15 mm wall) was sealed, by arc welding, and ~0.01 g of starting material was placed inside. Fluid-absent capsules were then placed in an oven at 110°C for at least 30 min and then sealed by arc welding. For fluid-present experiments, 0.7 μL of distilled, deionised H_2O were added to the capsules, by microsyringe, before sealing. Capsules were water-cooled during welding to prevent H_2O evaporation.

Experiments were carried out in a 12.7 mm diameter, non-end-loaded, piston–cylinder apparatus (Depths of the Earth Company, Cave Creek, AZ, USA). Experiments above 900°C used NaCl–Pyrex cells; all others used NaCl-only pressure cells. Most experiments used boron nitride (BN) packing around the capsule. BN is feebly permeable to H_2 and inhibits its diffusion into or out of the capsules (Truckenbrodt et al. 1997), keeping fH_2 and aH_2O at higher levels (and fO_2 at lower levels) than in experiments without BN. Thermocouples were type-K (chromel–alumel). The distance between the thermocouple and the sample capsule was minimised to prevent T uncertainties due to thermal gradients. Temperatures were controlled to ±1°C and are probably accurate to ±5°C. Pressures were recorded by a factory-calibrated strain gauge. Precision in pressure control varied but was generally around ±0.05 GPa.

The cylinder was lightly lubricated with MoS_2 grease before the sample assembly (wrapped in Pb foil) was

inserted. Before switching on the furnace, the whole assembly was pressurised to 1.2 GPa. Experiments below 1.0 GPa were left at this pressure for at least 30 min, to compact the furnace assembly. The pressure was then reduced to the desired value.

For the duration of an experiment, a compromise needs to be struck between shorter run times, characterised by smaller crystals and some disequilibrium (especially in the plagioclase compositions) and longer run times, with the danger of sample dehydration and departure from equilibrium melt proportions and compositions (e.g. Patiño Douce and Beard 1994). Run durations were 20–234 h, depending on the P and T. These durations were based on our experience of what is necessary to obtain near-equilibrium conditions and crystal growth to a reasonable size for analysis, without risking significant H_2O loss from the melts. They are similar to those used by Patiño Douce (2005) in a recent study of fluid-absent tonalite melting. Limited numbers of true reversal experiments have been undertaken using fluid-absent conditions. Beard and Lofgren (1991) concluded that 96 h was sufficient to approach equilibrium in partial melting experiments at $T \geq 900$°C. Patiño Douce (1995), Patiño Douce and Beard (1995) and Patiño Douce and Harris (1998) showed that equilibrium is generally approached. Where there is evidence of some disequilibrium in our experiments, we discuss this. Based on previous studies of the redox conditions in this piston-cylinder apparatus, log fO_2 is believed to lie between QFM and QFM-2 (Graphchikov et al. 1999).

Experiments were terminated by switching off the furnace while maintaining constant pressure until the solidus temperature was reached. This prevented exsolution of volatiles from any glass present, and sample vesiculation. Quenches took a few seconds, and signs of quench crystallisation (e.g. large skeletal crystals or microlite sprays) were not encountered. When the runs were completed, the capsules were removed from the cells, cleaned, opened and the contents examined. The samples were hand-ground in an agate mortar and optical grain mounts made. A single piece of the run product (or in some cases some powder) was mounted in epoxy resin and polished for analysis with the SEM/microprobe.

Analytical methods

The compositions of the experimental melts are of prime importance; analyses of the crystalline phases are of secondary interest. The generally small sizes of the melt pockets in fluid-absent runs at 800 and 850°C thus necessitated the use of a finely focussed electron beam for analysis. As is well known, during analysis of hydrous glasses, this results in counting losses on Na. To counter this, all glasses were analysed using the Microprobe at Manchester University, fitted with a cryostage at liquid N_2 temperature (–197°C). This limits both diffusion and volatilisation of elements with low atomic number, and essentially eliminates Na counting losses. As a test of the technique, Vielzeuf and Clemens (1992) analysed $NaAlSi_3O_8$ glass carrying 9 wt.% H_2O, with a fully focussed electron beam and live counting times of 100 s. With the sample at liquid N_2 temperature, and using a relatively low beam current, they obtained analyses with albite stoichiometry, indicating negligible Na counting losses. The same technique and conditions were used in the present study.

All mineral analyses were carried out on the JEOL 6310 SEM, fitted with an Oxford Instruments ISIS EDS system, at Kingston University, London. The chips of experimental run products did not always take a perfectly flat, level polish, resulting in variable absorption of emitted X-rays, depending on the angle of the surface relative to the collector. Thus, analytical totals were sometimes significantly <100% for anhydrous phases. In Appendix A (electronic supplementary material), totals are normalised to 100 wt.% for anhydrous phases and 92 and 96 wt.%, respectively, for amphiboles and micas. We also provide the original microprobe totals. The stoichiometry is generally good and the data are sufficiently robust to derive parameters such as Mg# in mafic phases and mol% An in plagioclase.

Results

Experimental conditions and run products are shown in Tables 4, 5. Appendices A and B (lodged as electronic supplementary materials) contain the electron probe analyses of all crystalline and glass phases (respectively). The results are discussed below.

Fluid-absent experiments

The solidus and biotite breakdown in SC5

Very small quantities of glass can be detected by the non-friable texture and brittleness of the run products when being crushed. Using this technique we can locate the solidus to within a few degrees. At 0.8 GPa and 800°C (SC5-3 and SC5-10) there is a small quantity of glass, slightly more in SC5-10. The increased melt proportion illustrates the effect of BN around the sample capsule (see above). Nevertheless, the amount

Table 4 Experimental conditions and run products for SC5 (biotite tonalite)

Run number	*P* (MPa)	*T* (°C)	Duration (h)	Fluid conditions	Run products	Comments
SC5-17	611 ± 30	680 ± 1	211	$XH_2O = 1$	Qtz, Pl, Bt, Kfs, Ilm	BN packing
SC5-9	599 ± 46	690 ± 1	193	$XH_2O = 1$	Gl, Qtz, Pl, Bt, Kfs, Ilm	BN packing
SC5-8	593 ± 47	700 ± 1	170	$XH_2O = 1$	Gl, Qtz, Pl, Bt, Ilm	BN packing
SC5-5	563 ± 33	700 ± 1	234	$XH_2O = 1$	Gl, Qtz, Pl, Bt, Ilm	
SC5-6	606 ± 30	720 ± 1	168	$XH_2O = 1$	Gl, Qtz, Pl, Bt, Ilm	
SC5-3	824 ± 13	800 ± 1	192	Fluid-absent	(Gl), Qtz, Pl, Bt, Kfs, Ilm	
SC5-10	808 ± 22	800 ± 1	221	Fluid-absent	Gl, Qtz, Pl, Bt, Kfs, Ilm	BN packing
SC5-2	836 ± 19	850 ± 1	127	Fluid-absent	Gl, Qtz, Pl, Bt, Opx, Ilm	
SC5-12	791 ± 18	850 ± 1	145	Fluid-absent	Gl, Qtz, Pl, Bt, Opx, Ilm	BN packing
SC5-16	792 ± 22	875 ± 1	122	Fluid-absent	Gl, Qtz, Pl, Bt, Opx, Ilm	BN packing
SC5-1	832 ± 28	900 ± 1	64	Fluid-absent	Gl, Qtz, Pl, Bt, Opx, ((Grt)), Ilm	
SC5-4	798 ± 19	950 ± 1	49	Fluid-absent	Gl, Qtz, Pl, Opx, ((Grt)), Ilm	NaCl + Pyrex cell
SC5-7	761 ± 21	950 ± 1	49	Fluid-absent	Gl, Qtz, Pl, (Bt), Opx, Ilm	NaCl + Pyrex cell, BN packing
SC5-14	750 ± 26	1,000 ± 1	46	Fluid-absent	Gl, Qtz, Pl, Opx, Ilm	NaCl + Pyrex cell, BN packing
SC5-20	882 ± 38	875 ± 1	123	Fluid-absent	Gl, Qtz, Pl, Bt, Opx, (Grt)	BN packing
SC5-18	974 ± 18	875 ± 1	119	Fluid-absent	Gl, Qtz, Pl, Bt, (Opx), Grt, Ilm	BN packing
SC5-19	1,101 ± 24	875 ± 1	143	Fluid-absent	Gl, Qtz, Pl, Bt, Opx, Grt, Ilm	BN packing
SC5-21	1,164 ± 20	800 ± 1	190	Fluid-absent	Gl, Qtz, Pl, Bt, Kfs, (Grt)	BN packing
SC5-13	1,185 ± 33	875 ± 1	123	Fluid-absent	Gl, Qtz, Pl, Bt, (Opx), Grt, Ilm	BN packing
SC5-24	1,213 ± 15	950 ± 1	20	Fluid-absent	Gl, Qtz, Pl, Bt, Opx, Grt	NaCl + Pyrex cell, BN packing

Phases in brackets are present in small quantities; phases in double brackets are present in trace quantities

Table 5 Experimental conditions and run products for SC4 (hornblende tonalite)

Run number	*P* (MPa)	*T* (°C)	Duration (h)	Fluid conditions	Run Products	Comments
SC4-14	595 ± 28	680 ± 1	216	$XH_2O = 1$	Gl, Qtz, Pl, Bt, Hbl, Ilm	BN packing
SC4-5	588 ± 22	700 ± 1	191	$XH_2O = 1$	Gl, Qtz, Pl, Bt, Hbl, Ilm	
SC4-4	590 ± 19	730 ± 1	168	$XH_2O = 1$	Gl, Qtz, Pl, Bt, Hbl, Ilm	
SC4-2	798 ± 21	850 ± 1	143	Fluid-absent	Gl, Qtz, Pl, Bt, Hbl, Opx, Mag, Ilm	
SC4-6	806 ± 20	850 ± 1	188	Fluid-absent	Gl, Qtz, Pl, Bt, Hbl, Cpx, Opx, Ilm	BN packing
SC4-7	791 ± 18	850 ± 1	145	Fluid-absent	Gl, Qtz, Pl, Bt, Hbl, Cpx, Opx, Ilm	BN packing
SC4-13	813 ± 19	875 ± 1	120	Fluid-absent	Gl, Qtz, Pl, Bt, Hbl, Cpx, Ilm	BN packing
SC4-1	794 ± 17	900 ± 1	75	Fluid-absent	Gl, (Qtz), Pl, Bt, Hbl, Cpx, (Ilm)	
SC4-3	823 ± 18	950 ± 1	48	Fluid-absent	Gl, Qtz, Pl, Bt, (Hbl), Cpx, Ilm	NaCl + Pyrex cell
SC4-10	758 ± 32	1,000 ± 1	48	Fluid-absent	Gl, Qtz, Pl, Bt, Cpx, Ilm	BN packing, NaCl + Pyrex cell
SC4-15	1,005 ± 26	875 ± 1	125	Fluid-absent	Gl, Qtz, Pl, Bt, Hbl, Cpx, Ilm	BN packing
SC4-16	1,082 ± 26	875 ± 1	123	Fluid-absent	Gl, Qtz, Pl, Bt, Hbl, Cpx, (Grt), Ilm	BN packing
SC4-12	1,215 ± 35	875 ± 1	123	Fluid-absent	Gl, Qtz, Pl, Bt, Hbl, Cpx, Grt, Ilm	BN packing
SC4-17	1,200 ± 27	800 ± 1	147	Fluid-absent	((Gl)), Qtz, Pl, Hbl, Kfs, Ilm	BN packing
SC4-18	1,176 ± 40	950 ± 1	46	Fluid-absent	Gl, Qtz, Pl, Hbl, Cpx, Ilm	BN packing, NaCl + Pyrex cell

Phases in brackets are present in small quantities; phases in double brackets are present in trace quantities

of melt is <5 vol.% in both experiments. Figure 2a shows SEM BSE images of these run products, with ~1 μm-wide glass pockets just visible at some grain intersections. These pockets are too small for accurate analysis. At 850°C (SC5-2 and SC5-12) there was slightly more melt, with pockets rarely large enough for analysis. At 875°C (SC5-16) there is considerably more glass (Fig. 2b).

Using the least squares mixing program Mix'n'Mac, phase proportions were calculated from the electron probe analyses and the bulk rock analysis of the starting material. Figure 3 shows how the phase proportions vary with *P* and *T*. These plots present the data produced using the software, moderated by analysis of the SEM images and visual estimates of mineral proportions in optical grain mounts. This correction

was necessary because the software occasionally overestimated the melt proportion. We do not have good control on the shape of the melt proportion curve (Fig. 3) at $T < 850$°C, so we simply assume linear growth of melt proportion, from a trace at 800°C to around 5% at 850°C.

In view of the small degree of melting at $T \leq 850$°C, and the rapid increase in melt proportion thereafter, it seems most likely that melting at $T < 850$°C involved a reaction other than biotite breakdown. The presence or absence of orthopyroxene in these runs would confirm the nature of the melting reaction. However, only small amounts of orthopyroxene would be predicted to form very close to the solidus, and this phase is difficult to distinguish optically from biotite in fine-grained run products. Orthopyroxene was confirmed by SEM analysis at 875°C, in run SC5-16. However, tiny crystals with low birefringence and straight extinction were visible in the grain mount of experiment SC5-2, at 850°C; these are inferred to be orthopyroxene. The beginning of biotite breakdown therefore lies just below 850°C.

Melting below 850°C is most probably due to reactions involving the small amounts of secondary epidote and sericitic mica present in the starting material. Such reactions with epidote could also involve biotite as a reactant, as in the Mg end-member reaction:

$$\text{Phl} + \text{Zo} + \text{Qtz} = \text{Ts} + \text{Kfs} + \text{Di} + \text{melt}. \quad (6)$$

This reaction occurs at lower temperatures than biotite breakdown to form orthopyroxene (Skjerlie and Johnston 1996). The main muscovite reactions are probably similar to:

$$\text{Ms} + \text{Qtz} + \text{Ab} = \text{Kfs} + \text{Al}_2\text{SiO}_5 + \text{melt}, \quad (7)$$

which also occurs at lower temperatures than biotite breakdown (Storre 1972; Storre and Karotke 1972; Petö 1976).

At 1.2 GPa and 800°C (experiment SC5-21), glass is present in the run product. Orthopyroxene is not present but there is a small quantity of garnet. The presence of garnet does not confirm biotite breakdown as it could be produced by melting involving epidote-group minerals, for example in the CMASH system:

$$\text{Zo} + \text{Qtz} = \text{Grs} + \text{An} + \text{melt}. \quad (8)$$

The solidus and hornblende breakdown in SC4

Glass was present in the products of all experiments on SC4. At 0.8 GPa the lowest-temperature fluid-absent experiment was at 850°C (SC4-6). Here, hornblende breakdown occurred by a reaction similar to:

$$\text{Hbl} + \text{Qtz} = \text{Cpx} + \text{Opx} + \text{melt}. \quad (9)$$

This reaction clearly begins below 850°C but, at 1.2 GPa and 800°C, there is only a tiny amount of glass in the run product. This melt probably formed through the breakdown of an epidote-group mineral and/or sericite, as inferred for SC5. At $P > 1$ GPa, orthopyroxene is not stable, and the solidus reaction instead produces garnet and clinopyroxene:

$$\text{Hbl} + \text{Qtz} = \text{Cpx} + \text{Grt} + \text{melt}. \quad (10)$$

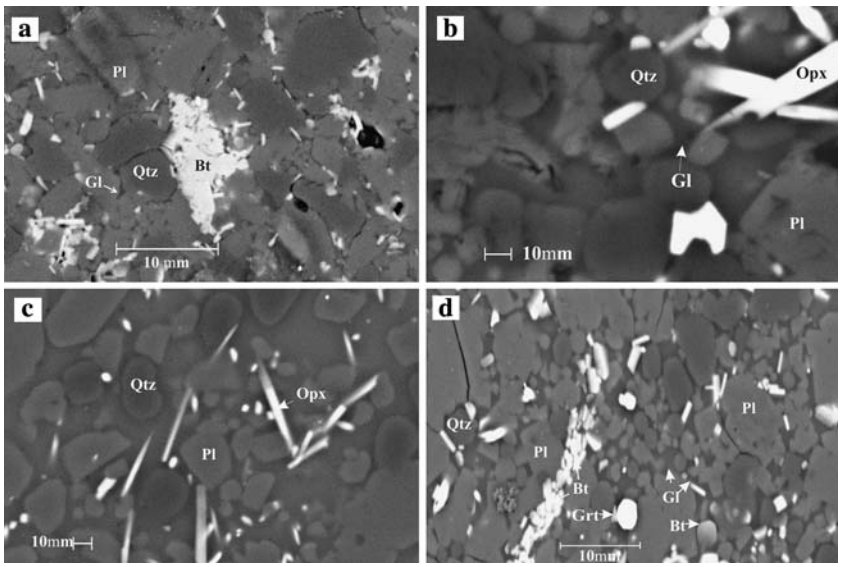

Fig. 2 Back-scattered electron SEM images of polished surfaces of run products from fluid-absent experiments on starting material SC5. **a** SC5-3 at ~0.8 GPa and 800°C, **b** SC5-16 at ~0.8 GPa and 875°C, **c** SC5-7 at ~0.8 GPa and 950°C and **d** SC5-20 at ~0.9 GPa and 875°C. Note the increasing melt proportion evident with increased T in the series at 0.8 GPa, and the appearance of garnet in the products of the 0.9 GPa experiment

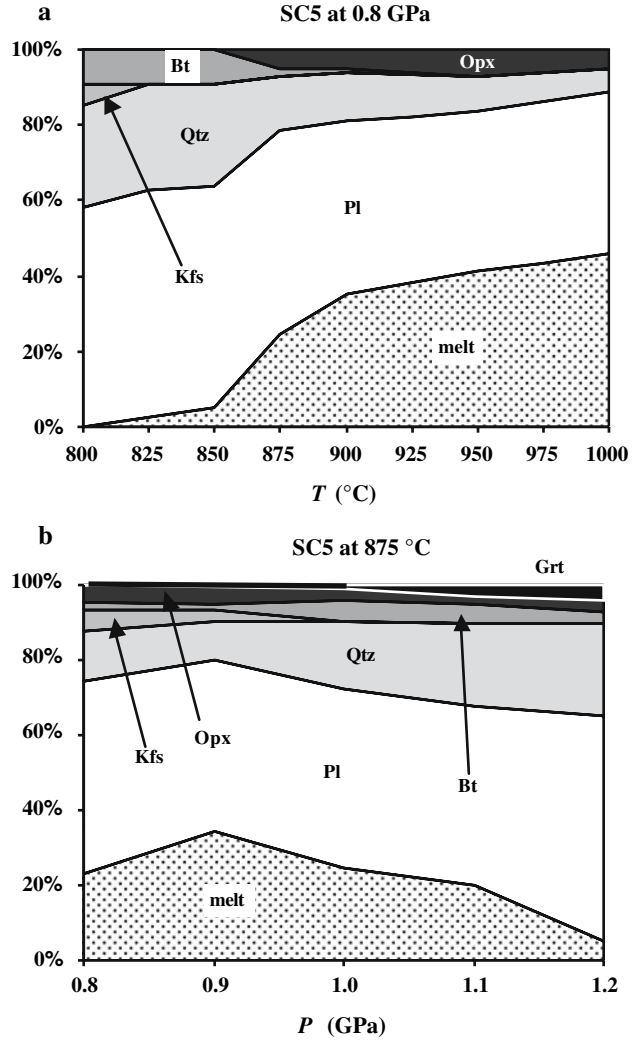

Fig. 3 Plots showing the variations of phase proportions in the products of fluid-absent experiments on starting material SC5, **a** as a function of *T* at 0.8 GPa, and **b** as a function of *P* at 875°C. Note that the very small amount of garnet present in run products at 900 and 950°C cannot be portrayed in the diagram. See, however, the phase diagram in Fig. 4 (**a**)

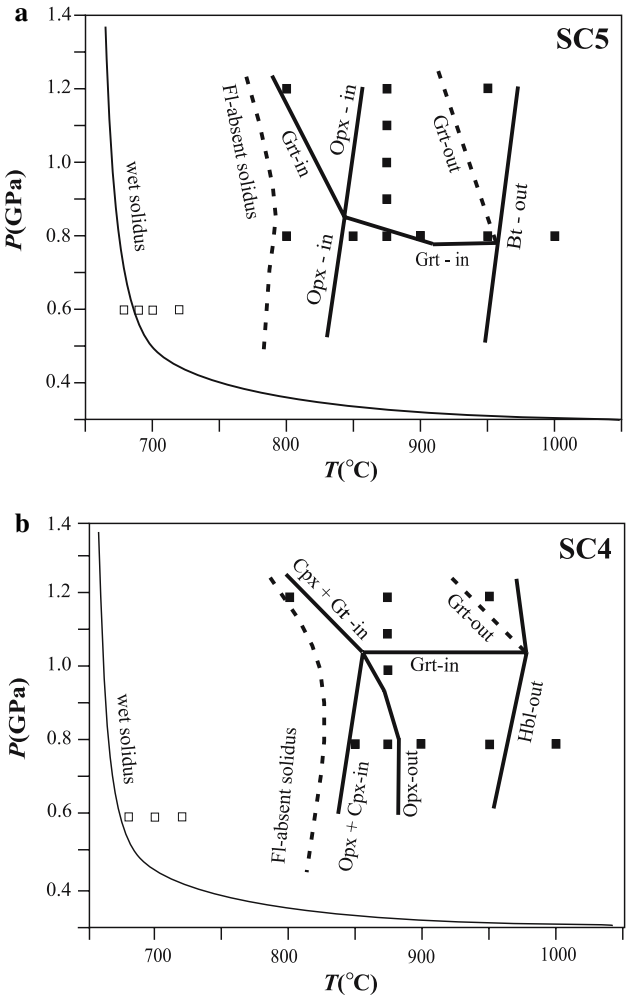

Fig. 4 *P–T* diagrams for partial melting of (**a**) SC5 and (**b**) SC4, derived from the experimental results, and showing the locations of major phase boundaries in biotite-dominated and hornblende-dominated tonalitic rocks, respectively. *Dashed lines* indicate less well-constrained phase boundaries. The shapes of the H_2O saturated solidi are approximate, and inferred from the shape of the wet solidus in the system Qtz-Ab-Or-H_2O. Note that the Kfs-out reaction lies very close to the Opx-in reaction, for both compositions

The restite would be garnet pyroxenite, rather than eclogite, as the pyroxenes are not omphacitic (<18 and mostly <11 mol% Jd component, Appendix A, Table A8). The CaTs contents of the clinopyroxenes are also very low (1–4 mol%, Appendix A, Table A8).

Fluid-absent partial melting in P–T sections

Figure 4 shows fluid-absent *P–T* diagrams for SC5 and SC4. Most of the phase boundaries are well constrained at 0.8 and 1.2 GPa. In SC5 there is a gradual decrease in orthopyroxene abundance with increasing *P*, accompanied by decreasing melt proportion. At 950°C, biotite is more abundant at 1.2 GPa than at 0.8 GPa, indicating a positive d*P*/d*T* slope for the Bt-out reaction. The presence of garnet at 1.2 GPa and 800°C indicates a negative d*P*/d*T* slope for the garnet-in reaction at $P > 0.8$ GPa in SC5. The major differences between the *P–T* diagram for biotite breakdown in SC5 and that for hornblende breakdown in SC4 are: the pressures of the Grt-in reactions, the absence of a clinopyroxene stability field in SC5 and the relatively small region for orthopyroxene stability in SC4. These differences reflect the contrasting mineralogies of the starting materials, but may seem surprising given the similar chemical compositions of SC4 and SC5. This point is discussed later.

Phase proportions and fertility of biotite tonalite (SC5)

In the first experiment at 0.8 GPa and 900°C (SC5-1), the melt fraction was small. However, this experiment did not use BN packing around the sample capsule. In the other experiments, the melt proportion increased gradually between 850 and 950°C (Fig. 3), up to 45 wt.% at 1,000°C. Very small but unquantified amounts of melt are produced at $T < 850$°C, as discussed earlier. Thus, if we are considering only melting by biotite and hornblende breakdown, the fertility figures need to be slightly reduced (perhaps up to 5%).

In run SC5-7 (at 950°C) a trace of biotite (<<1%) remained. However, the biotite crystals (identified from their shapes, contrast in BSE images and their optical properties in grain mounts) were too small for EMP analysis. At 1,000°C (SC5-14) biotite is absent. Thus, at 0.8 GPa, the Bt-out reaction lies just above 950°C. Quartz is consumed in the biotite melting reaction, and its modal abundance is halved at 875°C. The proportion then decreases more slowly up to 1,000°C, but residual quartz remains. Plagioclase abundance decreases slightly up to about 900°C and then remains approximately constant. Thus, the plagioclase content of the rock exerts only a secondary effect on melt formation. Since quartz is in excess, all the biotite should be capable of melting. Biotite abundance in the TTG protolith therefore exerts the primary control on the melt proportion, as predicted by Clemens and Vielzeuf (1987). K-feldspar is present at 800°C but disappears as soon as there is a significant proportion of melt (at 850°C). This phase is theoretically a product of fluid-absent biotite breakdown but is absent in most run products. The K_2O component is highly soluble in the melt, so that any K_2O not incorporated as $KAlSi_3O_8$ solid solution in plagioclase readily enters the melt. Apatite is commonly present in higher-temperature runs, confirming its position near the liquidus.

In SC5, at 0.8 GPa, small quantities of garnet are present at 900 and 950°C (runs SC5-1 and –4), but not at lower T. At 875°C, garnet is present at 0.9 GPa (run SC5-20) and abundant at $P \geq 1.0$ GPa. At 1.2 GPa, garnet is present at 800°C and abundant at 875°C (runs SC5-21 and –13) but absent at 950°C (run SC5-24), having been consumed in a melting reaction. At 875°C, the proportion of glass decreases with increasing P, with only a very small amount formed at 1.2 GPa. This is inferred to be due to the increased solubility of H_2O in the melt at higher P. Interestingly, the proportion of residual quartz increases with increasing P. This is probably a consequence of the growing importance of the garnet-forming reaction, which produces quartz. In the simple CMAS system, the analogous reaction is:

$$2\mathrm{En} + \mathrm{An} = \mathrm{Grt}_{(\mathrm{ss})} + \mathrm{Qtz}. \quad (11)$$

Another effect of increasing P is an increase in the thermal stability of biotite, which results in lower melt proportions. Comparing Fig. 2d (SC5-20, 0.9 GPa) with Fig. 2b (SC5-16, 0.8 GPa), it is apparent that biotite is the dominant mafic mineral at 0.9 GPa and orthopyroxene is uncommon. At a pressure only 0.1 GPa lower, orthopyroxene is a significant phase. This is due to the positive dP/dT slope of the biotite fluid-absent melting reaction.

Phase proportions and fertility of hornblende tonalite (SC4)

In SC4, the melt proportion increases steadily between 850 and 950°C (Figs. 5, 6), reaching 30% at 1,000°C. Due to its lower H_2O content, this hornblende tonalite is a little less fertile than the biotite tonalite (SC4). Orthopyroxene was identified in grain mounts of the experiments at 850°C (SC4-6 and –7) but the small size of the crystals and their low abundance prevented analysis. Clinopyroxene was also present in small amounts, though not in the more oxidising experiment (SC4-2) that lacked BN packing. Thus, the beginning of melting and the Cpx-in reaction are below but close to 850°C. Orthopyroxene is present in the products of experiments at 850°C and 0.8 GPa (SC4-2, –6 and –7). At higher T and P, orthopyroxene is not stable, probably due to a CMAS reaction similar to 11, above.

Quartz decreases dramatically in abundance over the interval of hornblende breakdown but is still present at the highest temperatures. As with the biotite tonalite, the proportion of hydrous mafic minerals that break down controls the quantity of melt. K-feldspar was not identified in the products of experiments carried out above the solidus, except in the 800°C experiment at 1.2 GPa (SC4-17), which was virtually at the solidus. Kfs is not formed through hornblende breakdown, and any K_2O component formed during the breakdown of the minor biotite in SC4 enters the melt within a few degrees of the solidus.

At 0.8 GPa, hornblende is present in all run products, except at 1,000°C (SC4-10), so the Hbl-out reaction lies between 950 and 1,000°C. The experiment at 950°C (SC4-3) was carried out without BN in the assembly. The consequent higher fO_2 would increase the thermal stability of both biotite and hornblende, through oxy-substitution. Nevertheless, only minor hornblende formed in SC4-3, and the Hbl-out reaction must lie only slightly above 950°C.

As in SC5, the melt proportion decreases with increasing P. Garnet formed at 1.1 and 1.2 GPa

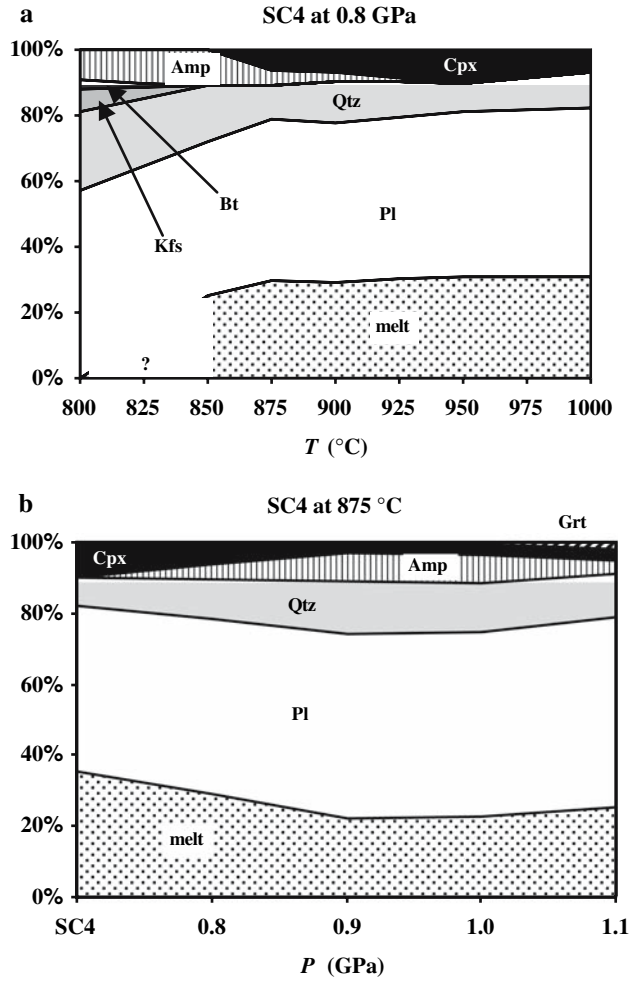

Fig. 5 Plots showing the variations of phase proportions in the products of fluid-absent experiments on starting material SC4, **a** as a function of *T* at 0.8 GPa, and **b** as a function of *P* at 875°C

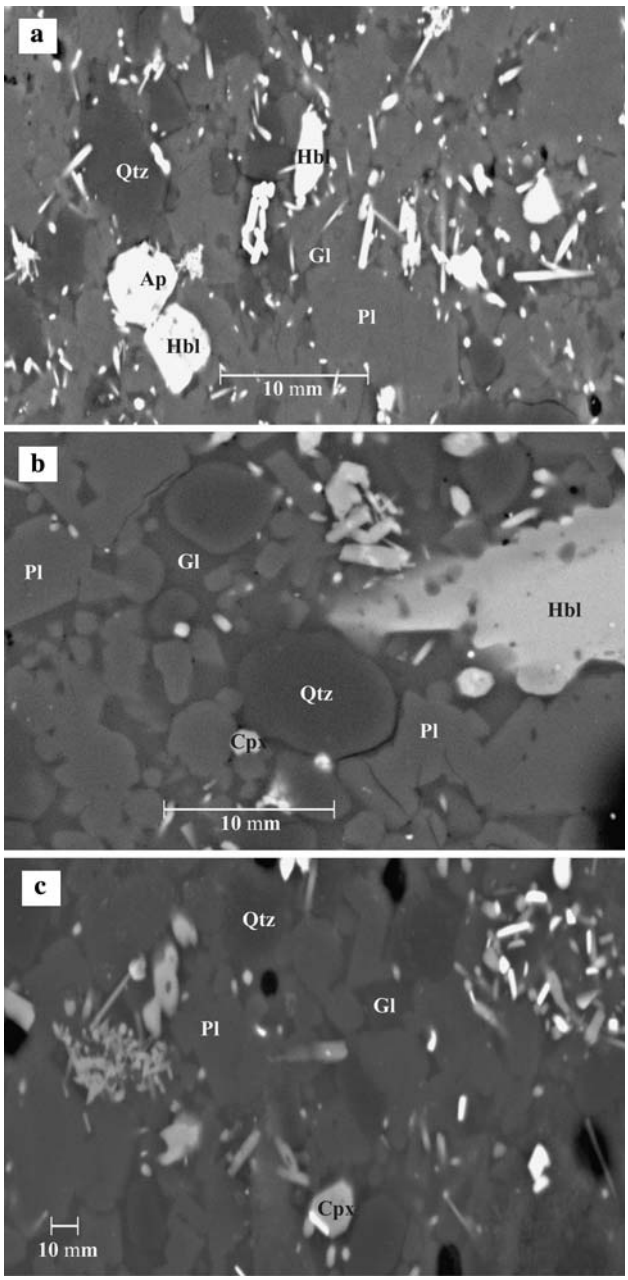

Fig. 6 Back-scattered electron SEM images of polished surfaces of run products from fluid-absent experiments on starting material SC4, at $P = 0.8$ GPa, **a** SC4-6 at 850°C, **b** SC4-1 at 900°C and **c** SC4-3 at 950°C. Note the appearance of clinopyroxene in the experiment at 900°C and the virtual disappearance of residual hornblende in the experiment at 950°C

(875°C), but not at any of the other conditions investigated. At 1.2 GPa and 875°C, about 6% garnet is present. In runs with garnet, pyroxene is much less abundant than at 0.8 GPa, and hornblende is the dominant mafic phase. At 1.2 GPa and 800°C (SC4-17) no garnet is present and clinopyroxene was tentatively identified in grain mounts (as tiny crystals with inclined extinction). At 950°C (SC4-18) garnet is again absent, and hornblende is scarce.

Compositions of restitic solids

We define restites as any mineral phases present in the run products, irrespective of whether they originated as subsolidus phases or were produced as reaction products. Analyses of restitic phases are presented in Appendix A, lodged as electronic supplementary material.

Plagioclase compositions (Tables A1 and A3) are not significantly different to those in the starting materials (An_{23}). However, in BSE images (e.g. Fig. 2a), the crystals have paler rims, ~1–2 μm wide, indicating some increase in An content. As in nature, the plagioclase is refractory, except for narrow rims that may have equilibrated with the melt. These rims

are too narrow for analysis. The lack of equilibration of the melt with the plagioclase is probably a factor in reducing melt production both in nature and the experiments. In nature, the problem seems to be quite severe, (Johannes 1984; Johannes et al. 1994).

The Mg# and Ti contents of restitic biotites generally increase and Al contents decrease with T (Tables A5 and A7). This is consistent with the results of Dooley and Patiño Douce (1996), who confirmed that Ti substitution in biotite increases its thermal stability. All the analysed amphiboles are hastingsitic hornblendes, with little variation in composition. Orthopyroxenes in the products of lower temperature (850°C) fluid-absent experiments on SC5 are En_{42} (Table A8). They become more magnesian with increasing T, reaching En_{63} at 1,000°C. All contain a significant Tschermak component. With increasing P, the orthopyroxenes become slightly more ferroan. The Na and Al contents of restitic clinopyroxenes (Table A8) do not vary systematically with T or P. At 0.8 GPa and 850–875°C, the clinopyroxenes are augitic, with Mg# = 59–66. With increasing T, Fe progressively replaces Ca, at constant Mg and, at 0.8 GPa and $T \geq 900$ C, the clinopyroxene is pigeonitic, with Mg# = 47–56. This is a relatively low T for pigeonite stability, lower than the inversion temperature (950–1,100°C) cited by Deer et al. (1992). Inversion temperature appears to be strongly pressure dependent, since experiments at $P \geq 1.0$ GPa produced pigeonite at T as low as 875°C. Neither Skjerlie and Johnston (1996) nor Singh and Johannes (1996b) noted pigeonite in their run products. However, Skjerlie and Johnston used a very different bulk starting composition, and Singh and Johannes used an experimental method that is considerably more prone to disequilibrium (see later).

At 1.1 GPa, the Pyp contents of garnets (Table A4) increase with T between 800 and 875°C, as predicted from the thermal stabilities of the garnet end members. The scarce garnets produced at 0.8 GPa have Grs contents <20 mol%. In SC5 garnets, the Grs component increases steadily with P, up to ~1.1 GPa, and then more rapidly to higher P. Garnets produced in experiments on SC4 have higher Grs contents (>20 mol%) than those produced in experiments on SC5. This is due to the different garnet-forming reactions in the two rocks. In SC4, the reaction consumes the Di component of clinopyroxene:

$$\mathrm{Di} + \mathrm{An} = \mathrm{MgCa_2Al_2Si_3O_{12}} + \mathrm{Qtz}\,(\mathrm{CMAS\ system}). \quad (12)$$

While, in SC5, the mafic reactant is an orthopyroxene, which produces a garnet with higher Mg/Ca:

$$2\mathrm{En} + \mathrm{An} = \mathrm{Mg_2CaAl_2Si_3O_{12}} + \mathrm{Qtz}\,(\mathrm{CMAS\ system}). \quad (13)$$

Thus, low-Grs garnets are stable at lower P and garnet can only be formed at $P < 1$ GPa if the tonalitic protoliths have biotite as the dominant mafic mineral. Ca partitioning between the garnet and the melt is probably responsible for the large variation in garnet compositions with P, with this same garnet-forming reaction. With increasing P, the solubility of Ca in garnet becomes greater than the solubility of Ca in the melt. Since there is little difference in bulk composition between the two starting materials (Table 2), it seems likely that the main control on garnet stability (at $P \leq 1.2$ GPa) is protolith mineralogy rather than bulk-rock composition.

Melt compositions

Average normalised analyses and CIPW norms of glasses are given in Appendix B (electronic supplementary material). All are peraluminous, typically with $SiO_2 > 70$ wt.%. Those produced from SC4 had between 0.13 and 2.01 wt.% normative c, while those from SC5 were more aluminous, with c between 0.91 and 2.44 wt.%. These differences reflect the fact that SC5 is mildly peraluminous while SC4 is metaluminous, a difference also reflected in garnet stability in the two starting materials. Partial melts can evolve towards peraluminous compositions by fractionation of hornblende and clinopyroxene (Cawthorn and Brown 1976; Abbott 1981). This is the most likely explanation for the peraluminous character of the melts from SC4, most of which coexisted with restitic hornblende and clinopyroxene.

Figure 7a shows a normative an-ab-or diagram, with field boundaries and rock names from Barker (1979). The rest of the plots in Fig. 7 include glasses from all experiments at 0.8 GPa (Fig. 7c, d), all experiments at 875°C, at varying P (Fig. 7b, e) and all H_2O-saturated experiments (Fig. 7f). Most fluid-absent experiments produced granodioritic and granitic melts. Glasses from experiments on SC4 generally have higher normative an than those in SC5 experiments but with similar normative or.

For SC5 experiments, normative or decreases and melt proportion increases with T (Fig. 7d). The melts have low normative an; those from experiments at ≥950°C have normative or/ab ≤ 0.67. Figure 8 shows a normative an-ab-or-q plot for glasses from SC5 experiments at 0.8 GPa and 875–1,000°C. With increasing T there is a slight trend of increasing normative ab, at the expense of q and or. The composition

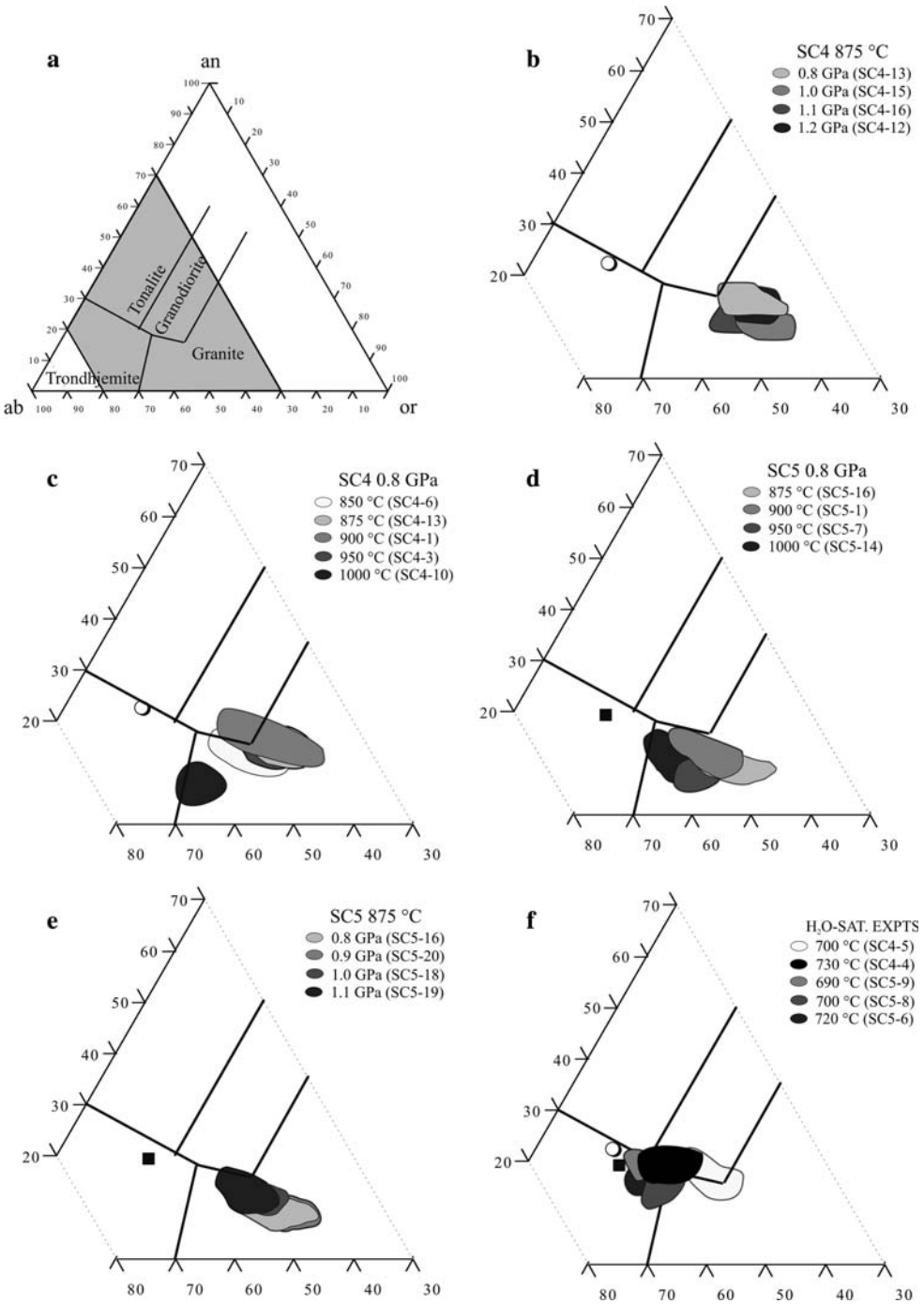

Fig. 7 Normative an-ab-or plots showing the compositional fields for glasses (quenched melts) formed in experiments on SC4 and SC5, as well as the compositions of the relevant starting materials (SC4 = *circle*, SC5 = *square*), **a** diagram showing the location of the field occupied by the other plots, and the rock names after Barker (1979), **b** SC4 glasses at 875°C, as a function of *P*, **c** SC4 glasses at 0.8 GPa as a function of *T*, **d** SC5 glasses at 0.8 GPa as a function of *T*, **e** SC5 glasses at 875°C as a function of *P*, and **f** glasses formed in fluid-present (H_2O-saturated) experiments at 0.6 GPa on SC4 and SC5

of the melt from SC5-1 is anomalous. However, without BN in the pressure cell, the conditions were rather more oxidising and the results are not comparable with the others. With inspection of the or-q-an field, it is clear that the main trend is towards ab, with very little variation in an. In general, the SC4 glass compositions do not vary greatly with *T*, though the melt produced at 1,000°C had low normative an. Due to increased solubility of the ferromagnesian component, the FeO contents of the glasses increase with increasing *T* (Appendix B).

Figure 7e shows an an-ab-or plot and Fig. 9 an an-ab-or-q diagram for SC5 melts formed at 875°C. With increasing *P*, normative or decreases, due to the increasing thermal stability of biotite—a consequence of the positive d*P*/d*T* of the Opx-in reaction. Thus, at higher *P*, there is less K_2O component available to dissolve in the melt. For SC4, there is no systematic

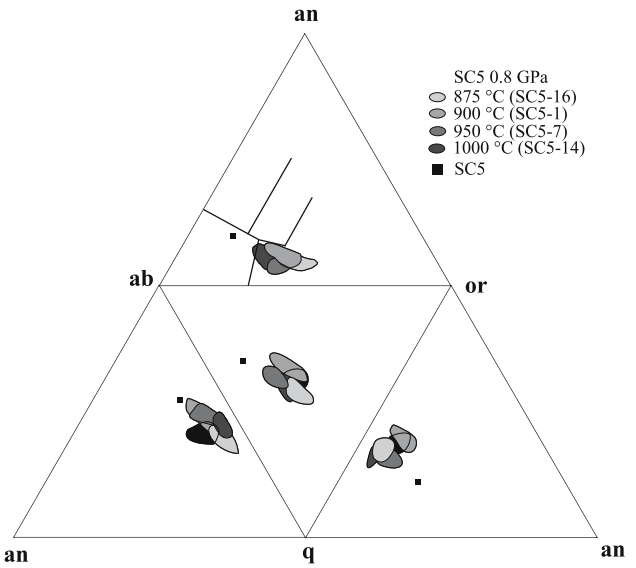

Fig. 8 Normative q-an-ab-or plot showing the compositions of glasses formed in fluid-absent experiments on SC5 at 0.8 GPa, with compositional fields in a-ab-or from Baker (1979)

variation in melt composition with *P*. Due to its low modal abundance, biotite stability is not a controlling factor in SC4. The thermal stability of both biotite and hornblende may increase at higher *P*, but this does not greatly affect the melt compositions.

As can be seen from Fig. 10, the experiments that produced melts with the highest normative or are also commonly those that produced melts with the highest normative q. The reason for the link between normative q and or is that the fluid-absent experiments were at relatively high *T*. At these conditions, most of the K_2O has already passed into the melt, and the relatively high-melt proportions mean that much of the quartz has also dissolved.

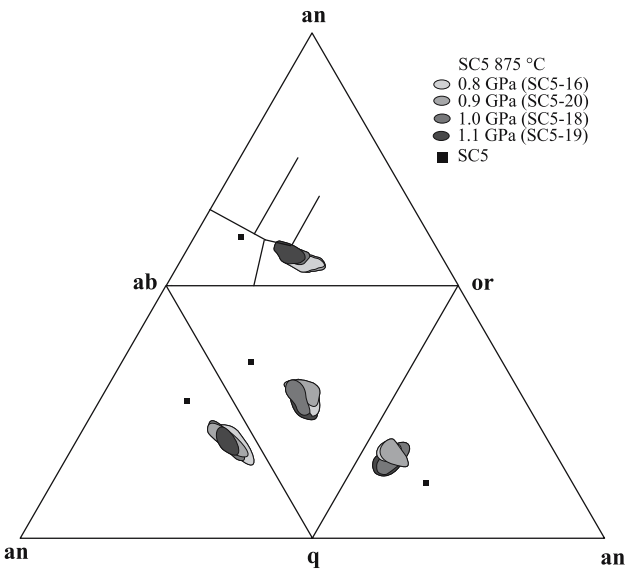

Fig. 9 Normative q-an-ab-or plot showing the compositions of glasses formed in fluid-absent experiments on SC5 at 875°C, with compositional fields in a-ab-or from Baker (1979)

Fluid-present (H_2O-saturated) experiments

Phase proportions

For all H_2O-saturated experiments, phase proportions were calculated using Mix'n'Mac. Figure 11 shows how these proportions vary with *T* (at 0.6 GPa). For SC5, the wet solidus lies between 680 and 690°C. At 690°C, glass appears in large quantities (>30%). There is a small decrease in the abundance of biotite, but quartz and plagioclase are the greatest contributors to the melt. The glass proportion increases to >40% at 720°C, again at the expense of quartz and plagioclase. Quartz remains stable at 730°C. Due to its low modal abundance and high-solubility in the melt, K-feldspar is stable only very close to the solidus.

The wet solidus for SC4 lies below 680°C. At 700°C plagioclase and quartz proportions are similar to those in SC5, but there is slightly less glass. At the solidus, a small amount of hornblende is consumed, but there is little further decrease in the mafic mineral content with increasing *T*. At 730°C (SC4-4), quartz is scarce, and

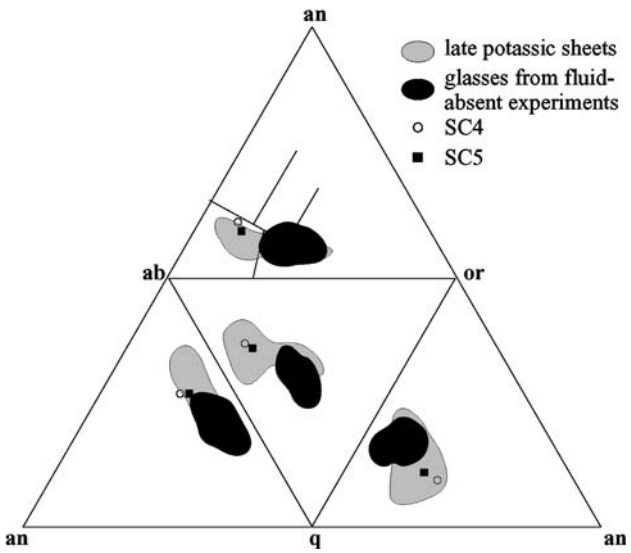

Fig. 10 Composite normative q-an-ab-or plot showing the compositional fields for glasses formed in all fluid-absent experiments on SC4 and SC5, compared with the fields for the late granitic sheets that intrude the Lewisian grey gneisses (analyses from H. R. Rollinson, written comm. 1997, Watkins 2002). The compositions of the starting materials are also marked

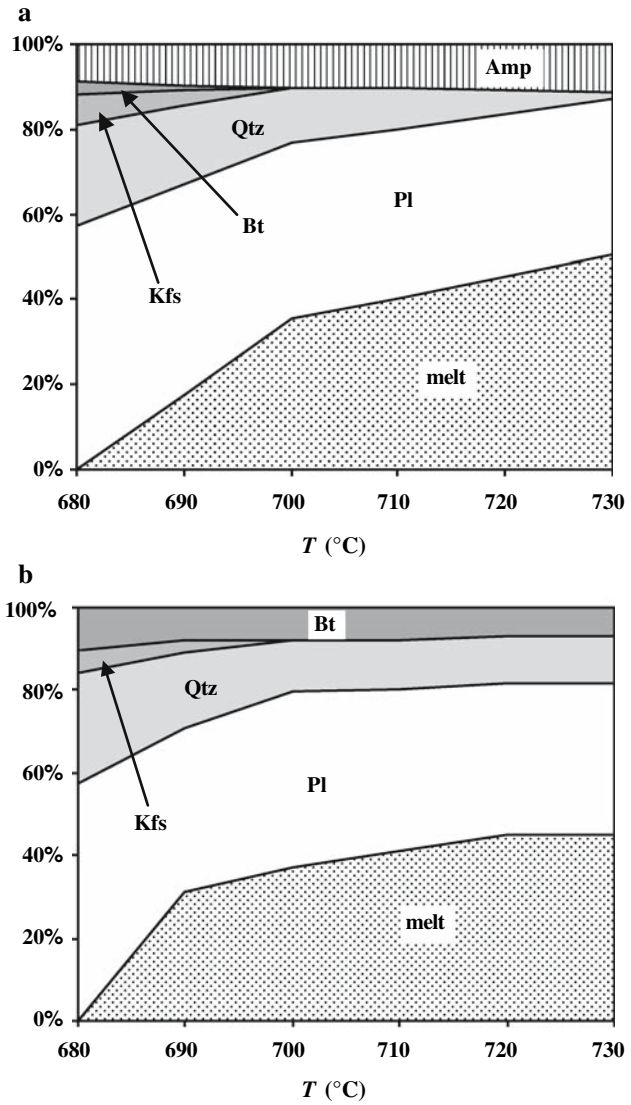

Fig. 11 Plots showing the variations of phase proportions in the products of fluid-present (H_2O-saturated) experiments on (**a**) SC4, and (**b**) SC5, as a function of *T* at 0.6 GPa

both hornblende and biotite remain stable. No new mineral phases appeared. Thus, the incongruent fluid-present biotite and hornblende breakdown reactions lie at >720 and >730°C, respectively.

Melts compositions

Figure 7f shows normative an-ab-or for all H_2O-saturated experiments, and Appendix B (electronic supplementary material) provides average melt compositions. The melts formed in the fluid-present experiments have considerably lower normative or and much higher normative c than the fluid-absent melts. There are two reasons for this. Most importantly, biotite remained stable in all the H_2O-saturated experiments on SC5, making less K_2O component available for the melt than in the fluid-absent experiments in which biotite breakdown occurred. More melt was produced in the H_2O-saturated experiments and the starting rock had limited K_2O. The experiment on SC4 at 700°C (SC4-5) produced melts with the highest normative or because the run was close to the solidus and at a *T* only just above the Kfs-out curve. Figure 12 shows normative q-an-ab-or compositions for all H_2O-saturated melts. As expected from published isobaric phase relations and modelling in simple granitic systems (e.g. Burnham and Nekvasil 1986) experiments at 690, 700 and 720°C produced similar melt compositions, with minimal scatter.

Discussion

Applicability of the fluid-absent experiments and comparisons with previous studies

Table 1 shows that the average Archaean felsic rock has $K_2O/Na_2O = 0.51$, rather higher than our starting materials (0.29 and 0.34). However, if we take the Barberton TTGs of southern Africa as typical of Archaean TTGs, these have K_2O/Na_2O in the range 0.23–0.55, with an average of 0.38 (Yearron 2003). Thus, the results for SC4 and SC5 are applicable to partial melting of relatively sodic Archaean TTGs,

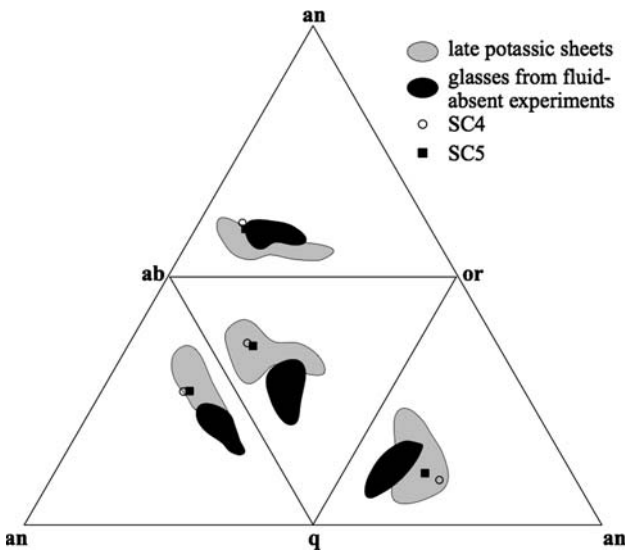

Fig. 12 Normative q-an-ab-or plot showing the compositional fields for glasses formed in fluid-present (H_2O-saturated) experiments on SC4 and SC5, compared with the fields for the late granitic sheets that intrude the Lewisian grey gneisses (as in Fig. 9). The compositions of the starting materials are also marked

which appear to be voluminous in some terranes. The most important primary findings of the present fluid-absent experiments are that:

1. Bt and Hbl melting both begin at about 850°C, with the incoming of pyroxenes.
2. The hydrous crystalline phases are consumed completely between 950 and 975°C.
3. Grt becomes stable at ~0.8 GPa for the biotite tonalite and ~1.0 GPa for the hornblende tonalite.
4. Melt proportions increase rapidly between 850 and 1,000°C, up to about 45%.
5. The melts are sodic granites to granodiorites and increase in K_2O/Na_2O and SiO_2 content at higher *P*.
6. The melts of the biotite tonalite are metaluminous while those of the hornblende tonalite are peraluminous.

Previous studies of fluid-absent melting of tonalitic starting materials were summarised earlier. Those most comparable to the present work are Patiño Douce and Beard (1995) and Skjerlie and Johnston (1996). There are general similarities in the locations of Px-in, Bt-out Px-out and Grt-in phase boundaries, and in the fertilities of the rocks, though melt production curves do vary considerably in shape and in the temperature of initial melting (Fig. 13).

Figure 14 shows plots of K_2O against SiO_2 for experimental glasses. Patiño Douce and Beard (1995) and Skjerlie and Johnston (1996) used starting materials with considerably lower SiO_2 (59–64 wt.%) than those used here (69–70 wt.%). From their synthetic biotite-rich gneiss and andesitic quartz amphibolite, Patiño Douce and Beard (1995) produced glasses with generally higher K_2O than in the present work. This is also true of the results of Castro (2004), and is due to the higher K_2O/Na_2O in their starting materials (0.37–2.82) compared with those of SC4 and SC5 (0.29 and 0.34). Skjerlie and Johnston (1996) also produced glasses with higher K_2O, for their F-rich biotite tonalite. Again, their starting material had $K_2O/Na_2O = 0.5$, considerably higher than in our starting materials. The results of Castro (2004) are puzzling in one respect—their low melt proportions. From our results, sodic metatonalites are somewhat more fertile as magma sources than more potassic types, albeit yielding much more sodic melts. Castro (2004) does not mention the durations of his experiments, so it is difficult to comment on the reason for the much lower fertility that he observed.

One lesson to be learned from this study is that rocks with only subtle chemical differences can develop quite different mineralogical compositions at the same metamorphic grade. These differences also lead to significant contrasts in phase relations and phase compositions during fluid-absent partial melting experiments. Thus, while true igneous crystallisation experiments, commonly starting with amorphous materials, are generally relevant to any rock or magma with similar chemistry, metamorphic and partial melting experiments, starting with crystalline materials, only have relevance to natural materials when the chemistry and the mineralogy of the rock and the experimental analogue are both similar.

TTG melting and the origin of potassic granites

The Lewisian Gneiss Complex as an example

The Archaean metamorphic rocks of the Lewisian Gneiss Complex form part of the North Atlantic Craton (Bridgewater et al. 1973). The dominant metatonalites, trondhjemites and granodiorites (TTGs) were emplaced at 3.03–2.68 Ga (Kinny and Friend 1997, 2005; Friend and Kinny 2001). Parts of the Complex were affected by granulite-facies metamorphism, mainly at 2.49 Ga (the Badcallian, Friend and Kinny 1995). From about 1.903 to 1.75 Ga (Lyon and Bowes 1977; Friend and Kinny 2001; Kinny and Friend 2005) a separate amphibolite-facies event, the Laxfordian, was associated with introduction of aqueous fluids, migmatisation and intrusion of late granite and pegmatite sheets.

As in most Archaean terranes, K-rich granitic plutons were emplaced after the main phase of TTG magmatism, and it has often been suggested that the potassic magmas were formed by 'reworking' (partial melting) of the TTGs. We chose our starting materials because they are typical of the amphibolite-facies sodic TTGs in many Archaean terranes. Such protoliths do not produce melts with sufficient K_2O to account for either the late granite sheets of the Lewisian or the voluminous, late, potassic granites in other Archaean terranes (e.g. the Barberton of South Africa and the Chilimanzi of Zimbabwe). The protoliths for the melts that formed the potassic granites must have had higher modal K-feldspar (or normative or) and less quartz. This corresponds with the conclusions of Castro (2004) who studied more potassic starting compositions and ruled them out, on the basis of their infertility rather than the melt compositions. Based on other partial melting experiments (see above), relatively potassic TTGs could generate greater volumes of granitic magma, provided that sufficiently high-temperatures were attained at crustal pressures.

Our experiments also show that H_2O-saturated partial melting of sodic TTGs could not produce the magmas that formed the later potassic series. The

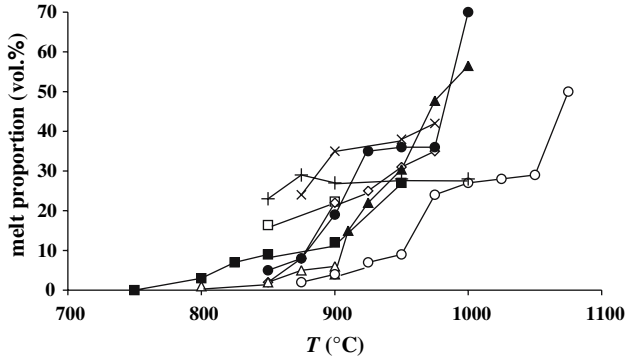

Fig. 13 Plot showing a compilation of experimentally derived *curves* for melt proportion (at ~1 GPa) as a function of *T*, for a variety of tonalitic starting compositions (modified from Fig. 8 of Clemens 2005). The experiments referred to are: Rutter and Wyllie (1988)—*Open diamonds*, Skjerlie and Johnston (1992, 1993)—*Open circles*, Singh and Johannes (1996a, b)—*Open squares*, Gardien et al. (1995)—*Open triangles* (BPQ I), *filled squares* (BPQ II), Patiño Douce and Beard (1995)—*Filled triangles*, Skjerlie and Johnston (1996)—*Filled circles*, present work—*crosses* + (SC4), crosses × (SC5)

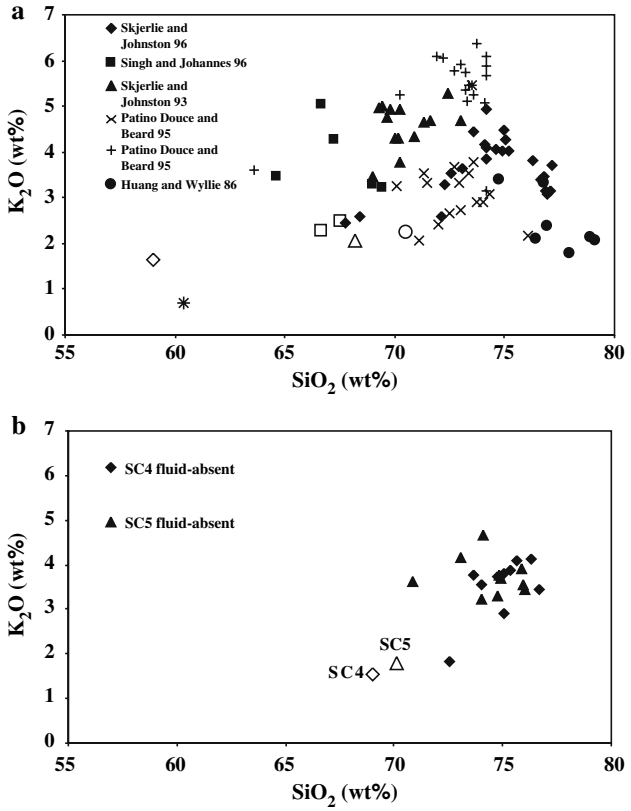

Fig. 14 K_2O versus SiO_2 Harker plots showing the compositions of fluid-absent partial melts, **a** formed in previous experimental studies, and **b** in the present work. The *open symbols* (and the *asterisk*) mark the compositions of the various starting materials, while the *filled symbols* and the *crosses mark* the melt compositions

protolith would have to have contained much more K_2O. However, it *would* be possible to generate granitic (sensu stricto) melts from the sodic TTGs at temperatures where biotite is no longer stable. Under fluid-present conditions, this could occur at reduced aH_2O and higher *T*, where orthopyroxene would become stable. However, such high-temperature fluid-present metamorphism is uncommon (see Clemens and Droop 1998 for recognition criteria). Indeed, as noted above, granulite-facies partial melting is generally fluid-absent. However seemingly interesting they may be, fluid-present melting models (e.g. Castro 2004) cannot explain the interdependency of *T* and melt H_2O content in felsic magmas (Scaillet et al. 1998; Clemens and Watkins 2001).

Crustal differentiation

Models for Archaean crustal differentiation commonly invoke partial melting of TTGs for the genesis of later Archaean granites (e.g. Anhaeusser 1981). The Barberton Mountainland, South Africa, is an oft-cited example of such a sequence of crustal evolution. Barberton consists of a greenstone belt, amphibolite-facies TTG gneisses and large K-rich batholiths. Moreover, the Dharwar, Zimbabwe and Slave cratons are all characterised by the emplacement of high-K monzogranitic plutons at the end of the Archaean (Bleeker 2003).

As noted above, melting of metatonalites and metatrondhjemites can only produce relatively sodic magmas, so there would be a problem in producing these large volumes of high-K magmas by fluid-absent partial melting of sodic metatonalites. Phase proportions and compositions in this and previous studies suggest that large volumes of restitic granulites would be formed, and the partial melts would be less potassic than the granites in these cratons (e.g. in Barberton, Meyer et al. 1994). Melts formed from some more potassic TTGs (e.g. Castro 2004; Patiño Douce 2005) are indeed granitic and much closer in composition to the late potassic granites. Nevertheless, the high-temperatures required (>900°C) and small melt proportions (<20%) suggest that, if this is the origin of the late potassic magmas, there must be very large volumes of granulite-facies felsic restite present at depth. This could be the case, but the deeper parts of these terranes are not commonly exposed, and the geophysical (rock density) evidence is unlikely to be definitive. The Lewisian is not the only Archaean terrane in which the TTGs are too sodic to be the protoliths for the late potassic granites. The Zimbabwe Craton contains late potassic granite sheets (kilometres in thickness) and

the TTGs have an average K_2O/Na_2O of just 0.37 (Luais and Hawkesworth 1994). As shown by Xiao and Clemens (2007), granitic magmas with K_2O/Na_2O ~1 can be produced by partial melting of relatively potassic, biotite-bearing TTGs, though only at pressures >2 GPa, in settings where there have been colossal degrees of crustal thickening. Such extreme thickening apparently did not occur in the Archaean. Thus, in many cases, late K-rich magmatism is unlikely to represent recycling of the regional TTG crust.

There are three possible origins for the late potassic granites in Archaean terranes. First, the TTGs may not be representative of Earth's earliest felsic crust. The geochemistry of TTGs, coupled with experimental work has shown that TTG-type melts are formed by partial melting of a variety of mafic granulitic to eclogitic sources (e.g. Martin 1987; Winther 1996; Condie 2005; Rapp et al. 2003). TTGs form about two thirds of the presently exposed Archaean crust (Jahn et al. 1984). Thus, it seems rather unlikely that the earliest felsic crust would have been greatly different from the TTGs. Second, the TTG terranes may tectonically overlie younger and more geochemically evolved crustal rocks. This is possible in some individual cases (e.g. Clemens et al. 2006), but is unlikely to be the general explanation. Finally, the late potassic magmas may contain a component derived from highly enriched mantle produced by reaction with fluids evolved during subduction of altered sea floor, with its sedimentary drape (see e.g. Rapp et al. 1999; Prouteau et al. 2001). The extremely potassic but magnesian sanukitoid magmas are thought to have originated in this way (e.g. Kovalenko et al. 2005). Mantle derivation of the high-K component may be an unconventional hypothesis, but this should be tested further, most easily using radiogenic isotope systems.

Acknowledgments The primary material for this paper is taken from the PhD thesis of JMW, supervised at Kingston University by JDC and PJT. Mr. W. Edwards and Mr. D. Plant are thanked for assistance with electron probe analysis at Kingston and Manchester, respectively. Access to the Manchester probe was provided through application to the then NERC-funded Facility. Dr. I. Cartwright (now at Monash University, Australia) provided JDC with the sample of experimental biotite tonalite SC5. Dr. S. Bignold is thanked for assistance in redrafting some of the figures. Earlier versions were reviewed by Dr. A. Patiño Douce and by Prof. S. Harley, who we thank for his constructive criticisms.

References

Abbott RN Jr (1981) AFM liquidus projection for granitic magmas with special reference to hornblende biotite and garnet. Can Mineral 19:103–110

Anhaeusser CR (1981) Barberton excursion guidebook: Archaean geology of the barberton mountainland. Geological Society of South Africa, Johannesburg, South Africa

Barboza SA, Bergantz GW (2000) Metamorphism and anatexis in the mafic complex contact aureole, Ivrea zone, northern Italy. J Petrol 41:1307–1327

Barker F (1979) Trondhjemite: definition environment and hypothesis of origin. In: Barker F (ed) Trondhjemites dacites and related rocks. Elsevier, Amsterdam, pp 1–12

Beard JS, Lofgren GE (1991) Dehydration melting and water-saturated melting of basaltic and andesitic greenstones and amphibolites at 1, 3, and 6.9 kb. J Petrol 32:365–401

Bleeker W (2003) The late Archean record: a puzzle in ca. 35 pieces. Lithos 71:99–134

Bridgewater D, Watson JV, Windley BF (1973) The Archaean craton of the north Atlantic region. Philos Trans R Soc A 273:493–512

Brown GC, Fyfe WS (1970) The production of granitic melts during ultrametamorphism. Contrib Mineral Petrol 28:310–318

Burnham CW, Nekvasil H (1986) Equilibrium properties of granite pegmatite magmas. Am Mineral 71:239–263

Castro A (2004) The source of granites: inferences from the lewisian complex. Scott J Geol 40:49–65

Cawthorn RG, Brown PA (1976) A model for the formation and crystallisation of corundum normative calc-alkaline magmas through amphibole fractionation. J Geol 84:467–476

Clemens JD (1984) Water contents of intermediate to silicic magmas. Lithos 17:273–287

Clemens JD (1990) The granulite—Granite connexion. In: Vielzeuf D, Vidal P (eds) Granulites and crustal differentiation. Kluwer, Dordrecht, pp 25–36

Clemens JD (2003) Melting of the continental crust I: fluid regimes, melting reactions and source-rock fertility. In: Brown M, Rushmer T (eds) Evolution and differentiation of the continental crust. Cambridge University Press, Cambridge (in press)

Clemens JD (2005) Melting of the continental crust I: fluid regimes, melting reactions and source-rock fertility. In: Brown M, Rushmer T (eds) Evolution and differentiation of the continental crust. Cambridge University Press, Cambridge pp 297–331

Clemens JD, Droop GTR (1998) Fluids, P-T paths and the fates of anatectic melts in the Earth's crust. Lithos 44:21–36

Clemens JD, Vielzeuf D (1987) Constraints on melting and magma production in the crust. Earth Planet Sci Lett 86:287–306

Clemens JD, Watkins JM (2001) The fluid regime of high-temperature metamorphism during granitoid magma genesis. Contrib Mineral Petrol 140:600–606

Clemens JD, Yearron LM, Stevens G (2006) Barberton (South Africa) TTG magmas: geochemical and experimental constraints on source-rock petrology, pressure of formation and tectonic setting. Precambrian Res 151:53–78

Condie KC (1997) Plate tectonics and crustal evolution. Butterworth-Heinemann, Oxford

Condie KC (2005) TTGs and adakites: are they both slab melts? Lithos 80:33–44

Deer WA, Howie RA, Zussman J (1992) An Introduction to the rock forming minerals, 2nd edn. Longman Scientific and Technical, pp 696, Harlow, Essex, UK

Dooley DF, Patiño Douce A (1996) Fluid-absent melting of F-rich phlogopite + rutile + quartz. Am Mineral 81:202–212

Dziggel A, Stevens G, Poujol M, Anhaeusser CR, Armstrong RA (2002) Metamorphism of the granite-greenstone terrane south of the Barberton greenstone belt, South Africa: and

insight into the tectono-thermal evolution of the 'lower' portions of the onverwacht group. Precambrian Res 114:221–247

Friend CRL, Kinny PD (1995) New evidence for protolith ages of lewisian granulites northwest Scotland. Geology 23:1027–1030

Friend CRL, Kinny PD (2001) A reappraisal of the lewisian gneiss complex: geochronological evidence for tectonic assembly of disparate terranes in the proterozoic. Contrib Mineral Petrol 142:198–218

Fyfe WS (1973) The granulite facies, partial melting and the Archean crust. Phil Trans R Soc Lond A273:457–461

Gardien V, Thompson AB, Grujic D, Ulmer P (1995) Experimental melting of biotite + plagioclase + quartz ± muscovite assemblages and implications for crustal melting. J Geophys Res-solid Earth 100:15581–15591

Gardien V, Thompson AB, Ulmer P (2000) Melting of biotite + plagioclase + quartz gneisses: the role of H_2O in the stability of amphibole. J Petrol 41:651–666

Graphchikov AA, Konilov AN, Clemens JD (1999) Biotite dehydration, partial melting, and fluid composition: experiments in the system $KAlO_2$–FeO–MgO–SiO_2–H_2O–CO_2. Am Mineral 84:15–26

Guernina S, Sawyer EW (2003) Large-scale melt-depletion in granulite terranes: an example from the Archean Ashuanipi subprovince of Quebec. J Metamorphic Geol 21:181–201

Jahn BM, Vidal P, Kröner A (1984) Multichronometric ages and origin of Archaean tonalitic gneisses in Finnish Lapland: a case for long crustal residence time. Contrib Mineral Petrol 86:398–408

Johannes W (1984) Beginning of melting in the granite system Qz–Or–Ab–An–H_2O. Contrib Mineral Petrol 86:264–273

Johannes W, Bogolepov M, Behrens H (1994) Melting kinetics and equilibrium compositions in the systems Qz–Ab–An–H_2O and Qz–Ab–An–Al_2O_3–H_2O. Terra Nova (Abstract Suppl) 1:26

Kinny PD, Friend CRL (1997) U-Pb isotopic evidence for the accretion of different crustal blocks to form the lewisian complex northwest Scotland. Contrib Mineral Petrol 129:326–340

Kinny PD, Friend CRL (2004) Proposal for a terrane-based nomenclature for the Lewisian Gneiss complex of NW Scotland. J Geol Soc London (in press)

Kinny PD, Friend CRL (2005) Proposal for a terrane-based nomenclature for the Lewisian Gneiss complex of NW Scotland. J Geol Soc London 162:175–186

Kovalenko A, Clemens JD, Savatenkov V (2005) Petrogenetic constraints for the genesis of Archaean sanukitoid suites: geochemistry and isotopic evidence from Karelia, Baltic Shield. Lithos 79:147–160

Luais B, Hawkesworth CJ (1994) The generation of continental-crust—An integrated study of crust-forming processes in the Archean of Zimbabwe. J Petrol 35:43–93

Lyon TDB, Bowes DR (1977) Rb-Sr, U-Pb and K-Ar isotopic study of the lewisian complex between durness and loch laxford Scotland. Krystalinikum 13:53–72

Martin H (1987) Petrogenesis of Archaean trondhjemites, tonalites and granodiorites from Eastern Finland: major and trace element geochemistry. J Petrol 28:921–953

McGregor VR (1979) Archean grey gneisses and the origin of the continental crust: evidence from the Gothab region West Greenland. In: Barker F (ed) Trondhjemites dacites and related rocks. Elsevier, Amsterdam, pp 1–12

Meyer FM, Robb LJ, Reimold WU (1994) Contrasting low-Ca and high-Ca granites in the Archaean Barberton mountain land Southern Africa. Lithos 32:63–76

Patiño Douce AE (1995) Experimental generation of hybrid silicic melts by reaction of high-Al basalt with metamorphic rocks. J Geophys Res Solid Earth 100(B8):15623–15639

Patiño Douce AE (1999) What do experiments tell us about the relative contribution of crust and mantle to the origin of granitic magmas. In: Castro A, Fernández C, Vigneresse J-L (eds) Understanding granites: integrating new and classical techniques. Geological Society Special Publication No 168, The Geological Society, London, pp 55–75

Patiño Douce AE (2005) Vapor-absent melting of tonalite at 15–32 kbar. J Petrol 46:275–290

Patiño Douce AE, Beard JS (1994) H_2O loss from hydrous melts during fluid-absent piston-cylinder experiments. Am Mineral 79:585–588

Patiño Douce AE, Beard JS (1995) Dehydration-melting of biotite gneiss and quartz amphibolite from 3 to 15 kbar. J Petrol 36:707–738

Patiño Douce AE, Harris N (1998) Experimental constraints on Himalayan anatexis. J Petrol 39:689–710

Petford N, Gallagher K (2001) Partial melting of mafic (amphibolitic) lower crust by periodic influx of basaltic magma. Earth Planet Sci Lett 193:483–499

Petö P (1976) An experimental investigation of melting relations involving muscovite and paragonite in the silica-saturated portion of the system K_2O–Na_2O–Al_2O_3–SiO_2–H_2O. Prog Exp Petrol 3:41–45

Prouteau G, Scaillet B, Pichavant M, Maury R (2001) Evidence for mantle metasomatism by hydrous silicic melts derived from subducted oceanic crust. Nature 410:197–200

Rapp RP, Shimizu N, Norman MD, Applegate GS (1999) Reaction between slab-derived melts and peridotite in the mantle wedge: experimental constraints at 3.8 GPa. Chem Geol 160:335–356

Rapp RP, Shimizu N, Norman MD (2003) Growth of early continental crust by partial melting of eclogite. Nature 425:605–608

Rutter MJ, Wyllie PJ (1988) Melting of vapour-absent tonalite at 10 kbar to simulate dehydration-melting in the deep crust. Nature 331:159–160

Scaillet B, Holtz F, Pichavant M (1998) Phase equilibrium constraints on the viscosity of silicic magmas—1. Volcanic-plutonic association. J Geophys Res Solid Earth 103:27257–27266

Singh J, Johannes W (1996a) Dehydration melting of tonalites. 1. Beginning of melting. Contrib Mineral Petrol 125:16–25

Singh J, Johannes W (1996b) Dehydration melting of tonalites. 2. Compositions of melts and solids. Contrib Mineral Petrol 125:26–44

Skjerlie KP, Johnston AD (1992) Vapor-absent melting at 10-kbar of a biotite-bearing and amphibole bearing tonalitic gneiss—Implications for the generation of A-type granites. Geology 20:263–266

Skjerlie KP, Johnston AD (1993) Fluid-absent melting behaviour of an F-rich tonalitic gneiss at mid-crustal pressures: implications for the generation of anorogenic granites. J Petrol 34:785–815

Skjerlie KP, Johnston AD (1996) Vapour-absent melting from 10 to 20 kbar of crustal rocks that contain multiple hydrous phases: implications for anatexis in the deep to very deep continental crust and active continental margins. J Petrol 37:661–691

Storre B (1972) Dry melting of muscovite + quartz in the range Ps = 7 kb to Ps = 20 kb. Contrib Mineral Petrol 37:87–89

Storre B, Karotke E (1972) Experimental data on melting reactions of muscovite + quartz in the system K_2O–Al_2O_3–

SiO_2–H_2O to 20 kb water pressure. Contrib Mineral Petrol 36:343–345

Taylor SR, McLennan SM (1985) The continental crust: its composition and evolution. Blackwell, Oxford, pp 312

Truckenbrodt J, Ziegenbein D, Johannes W (1997) Redox conditions in piston-cylinder apparatus: the different behavior of boron nitride and unfired pyrophyllite assemblies. Am Miner 82:337–344

Vielzeuf D, Clemens JD (1992) Fluid-absent melting of phlogopite + quartz: experiments and models. Am Mineral 77:1206–1222

Watkins JM (2002) Crustal melting processes and the formation of granulites and granites: a study based on the lewisian complex, NW Scotland. Ph.D. (unpubl.) thesis, Kingston University, 355 pp

Wells PRA (1981) Accretion of continental crust: thermal and geochemical consequences. Phil Trans R Soc London A 301:347–357

White AJR, Chappell BW (1977) Ultrametamorphism and granitoid genesis. Tectonophysics 43:7–22

Winther KT (1996) An experimentally based model for the origin of tonalitic and trondhjemitic melts. Chem Geol 127:43–59

Xiao L, Clemens JD (2007) Origin of potassic (C-type) adakite magmas: experimental and field constraints. Lithos (in press)

Yearron LM (2003) Archaean granite petrogenesis and implications for the evolution of the Barberton mountain land, South Africa. Ph.D. (unpubl.) thesis, Kingston University, 352 pp